Monthly Notices
of the
ROYAL ASTRONOMICAL SOCIETY

MNRAS **494,** 62–68 (2020)
Advance Access publication 2020 March 13

doi:10.1093/mnras/staa689

2MASS J15460752−6258042: a mid-M dwarf hosting a prolonged accretion disc

Jinhee Lee [1,2] Inseok Song [2★] and Simon Murphy [3]

[1] *School of Space Research, Kyung Hee University, 1732, Deogyeong-Daero, Giheung-gu, Yongin-shi, Gyuonggi-do 17104, South Korea*
[2] *Department of Physics and Astronomy, The University of Georgia, Athens, GA 30602, USA*
[3] *School of Science, University of New South Wales Canberra, ACT 2611, Australia*

Accepted 2020 February 28. Received 2020 February 28; in original form 2019 August 29

ABSTRACT

We report the discovery of the oldest (∼55 Myr) mid-M type star known to host ongoing accretion. 2MASS J15460752–6258042 (2M1546, spectral type M5, 59.2 pc) shows spectroscopic signs of accretion such as strong H α, He I, and [O I] emission lines, from which we estimate an accretion rate of $\sim 10^{-10}$ $M_\odot$ yr^{-1}. Considering the clearly detected infrared excess in all *WISE* bands, the shape of its spectral energy distribution (SED) and its age, we believe that the star is surrounded by a transitional disc, clearly with some gas still present at inner radii. The position and kinematics of the star from *Gaia* DR2 and our own radial-velocity measurements suggest membership in the nearby ∼55 Myr-old Argus moving group. At only 59 pc from Earth, 2M1546 is one of the nearest accreting mid-M dwarfs, making it an ideal target for studying the upper limit on the lifetimes of gas-rich discs around low-mass stars.

Key words: accretion, accretion discs – stars: late-type – stars: pre-main-sequence – open clusters and associations: individual.

1 INTRODUCTION

Stars inevitably harbour discs in the early stages of the star formation process and the lifetime of such discs is one of the most important parameters for understanding early stellar evolution. Moreover, because gas-giant planet formation must occur while the disc is gas rich, the disc lifetime is also a crucial parameter in planet formation scenarios. By surveying young (2–30 Myr) clusters, Haisch, Lada & Lada (2001) showed the lifetime of gas-rich discs is ∼2 Myr and ongoing accretion is rare beyond ages of ∼10 Myr. Mamajek (2009) noted that the disc dissipation time-scale should be dependent on the mass and hence spectral type (temperature) of the host star, and Ribas, Bouy & Merín (2015) showed that high-mass (>2 $M_\odot$) stars dispersed their discs up to twice as fast as lower mass stars.

Recently, several examples of circumstellar disc accretion at ages greater than ∼10 Myr have been identified (e.g. PDS 66 – 20 Myr; Mamajek, Meyer & Liebert 2002, HD 21197−30 Myr; Moór et al. 2011, 49 Ceti – 40 Myr; Zuckerman & Song 2012, *WISE* J080822.18−644357.3 – 45 Myr; Silverberg et al. 2016; Murphy, Mamajek & Bell 2018, J0446A and B, J0949A and B; Silverberg et al. 2020), and they have been treated as unusual anomalies without delving into the problem of prolonged gas accretion at extreme ages. In spite of the small number of cases, such old pre-MS stars hosting accretion discs can be challenging to the hypothesis for the rapid planet formation (Greaves & Rice 2010; Najita & Kenyon 2014; Manara, Morbidelli & Guillot 2018; Pfalzner & Bannister 2019) and provide the upper limit on the life times of gas-rich discs.

The young M5 star 2MASS J15460752–6258042 (hereafter 2M1546) was serendipitously found by us in a survey of low mass moving group candidate members from *Gaia* DR2 (Lee et al., in preparation). 2M1546 was first observed spectroscopically and classified as a T Tauri star with strong H α emission by Miszalski & Mikołajewska (2014) during their survey for new symbiotic stars selected from the AAO/UKST SuperCOSMOS H α Survey. In this work, we analyse optical spectra of 2M1546, its IR excess and spectral energy distribution (SED), and evaluate its age based on the kinematic membership of nearby young moving groups. From this analysis, we conclude that 2M1546 is the oldest (55 Myr) and one of the nearest (59 pc) accreting M-type stars discovered to date.

2 SPECTROSCOPIC OBSERVATIONS AND DATA ANALYSIS

We observed 2M1546 using the Wide Field Spectrograph (WiFeS; Dopita et al. 2007) mounted on the *ANU 2.3-m telescope* at Siding Spring Observatory during 2018 June and 2019 February. A summary of these observations is given in Table 1. The B3000 and R7000 gratings provided wavelength coverage of 3500–6000 Å ($\lambda/\Delta\lambda \sim 3000$) and 5300–7000 Å ($\lambda/\Delta\lambda \sim 7000$), respectively. The raw data were reduced using the PYTHON-based data reduction pipeline, PyWiFeS (Childress et al. 2014). The reduction process includes bad pixel repair, bias, and dark current subtraction, flat-

★ E-mail: song@uga.edu

Table 1. Summary of ANU 2.3-m/WiFeS observations of 2M1546.

UT date	MJD	Grating	SpT	RV (km s^{-1})	v_{10} [Hα] (km s^{-1})	Equivalent width (Å)[a] Hα	He I λ6678	[O I] λ6300	Li I λ6708
2018 Jun 4	58273.5813	R7000	M5	-4.4 ± 0.9	366	-210	-1.6	-3.6	0.43
2019 Feb 15	58529.6854	R7000 and B3000	M5	-3.5	310	-120	-0.8	-3.8	0.60

Note. [a]Negative values are in emission.

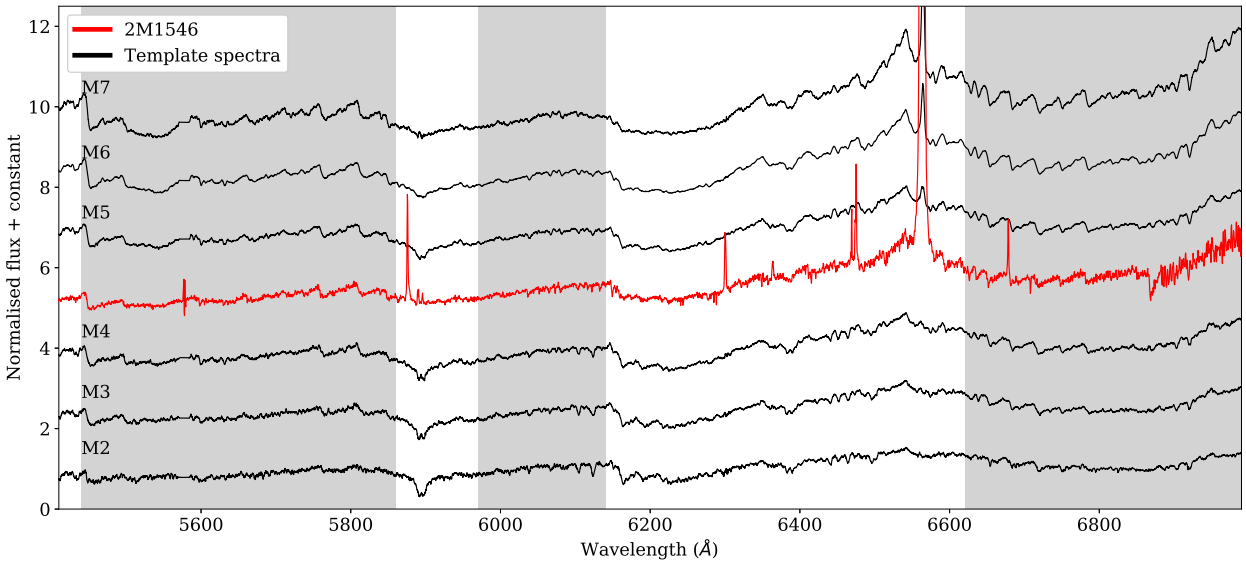

Figure 1. R7000 spectrum of 2M1546 (red) compared to the M-type templates from Bochanski et al. (2007). The templates are mean spectra of four thousand dwarfs from the SDSS (York et al. 2000). For details of creating these template spectra, see Bochanski et al. (2007). The spectrum of 2M1546 and the templates were normalized at 5800 Å prior to plotting. In the spectral type determination, the overall shape of the target and templates are compared focused more on the grey-shaded area.

fielding, wavelength calibration, flux calibration, and data cube creation. The wavelength calibration was performed using a series of Ne–Ar arc lamp exposures, taken throughout the night.

We compared the R7000 spectrum against the M-type spectral templates of Bochanski et al. (2007) that were generated by utilizing more than 4000 M-dwarfs spectra from the Sloan Digital Sky Survey (SDSS; York et al. 2000). Visual comparison of the 2M1546 spectra against a set of M-dwarf template spectra show the best match at M5. 2M1546 is located well outside of any molecular cloud and, at a distance of only 60 pc, it should have negligible interstellar extinction. Nevertheless, the accretion causes 'veiling', in which the accretion shock increases flux in the UV/optical, while the surrounding accretion disc produces additional flux to the photosphere in the IR (Vacca & Sandell 2011). Veiling can potentially affect our spectral type estimation because it will change the spectral shape (Herczeg & Hillenbrand 2008; Manara et al. 2013; Ingleby et al. 2014). However, a change in the spectral shape due to veiling occurs usually over a wide wavelength range while our spectral type estimate is focused on rather narrow wavelength ranges of 100–200 Å (e.g. shaded regions of Fig. 1). Therefore, our estimate of M5 spectral type should not be far from the truth and appropriate for the discussion in this paper. A more robust, unambiguous spectral type estimate can be done in the future by using a high spectral resolution echelle spectrum by measuring line ratios of some temperature sensitive lines that are adjacent in wavelengths so that veiling effect can be negligible.

The Li 6708 Å absorption feature was strongly detected in both epochs of WiFES spectra (EW of 430 and 600 mÅ). Considering a typical equivalent width measurement uncertainty (∼50 mÅ) in our WiFES spectra, the observed difference is likely a real variability of the Li 6708 line strength and related to a variable veiling. For an M5 star, the detected Li 6708 line strength indicates the undepleted level of Lithium in the atmosphere while a 'normal' 55 Myr old M5 star should have depleted all Lithium already. An ongoing accretion must have replenished Lithium in the atmosphere so that the 6708 line was strongly detected in our observation.

2.1 Emission lines

The magnetospheric accretion of the disc occurs from the inner edge of the disc on to the surface of the central source. This supersonic flow has nearly freefall velocities, resulting in large line widths of some emission lines. In the region of the accretion shock, on the other hand, some narrow emission lines are more likely produced (Hartmann, Herczeg & Calvet 2016). The strength and/or shape of some lines such as hydrogen recombination lines and He I, Ca II, and Na I lines are known as accretion tracers (see e.g. Muzerolle, Hartmann & Calvet 1998; Antoniucci et al. 2011; Biazzo et al. 2014). The observed spectra of 2M1546 cover Hα and He I lines.

Both WiFeS observations show strong Hα emission, with equivalent widths in excess of 100 Å. However, because of the contrast effect caused by the depression of the stellar continuum by molecular absorption, the equivalent widths of Hα lines (EW(Hα)) in non-accreting stars are typically enhanced at later spectral types (Basri & Marcy 1995; Martín et al. 1998; White & Basri 2003). Barrado y Navascués & Martín (2003) presented an EW(Hα) accretion criterion as a function of spectral type, where the upper limit for accretors is EW(Hα) ~ -20 Å at M5. This was corroborated by

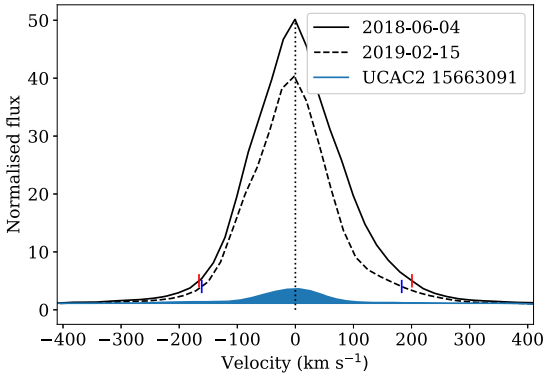

Figure 2. WiFeS/R7000 Hα velocity profiles of 2M1546. Small vertical lines (red and blue) indicate 10 per cent of the peak flux used for measuring the v_{10} value. The WiFeS line profile of the M5 non-accretor UCAC2 15663091 is also plotted for comparison. All spectra are shifted to the heliocentric rest frame.

Duchêne et al. (2017) after an extensive analysis of known T Tauri stars. With equivalent widths of −210 and −120 Å, 2M1546 clearly exceeds this criterion.

Although the contrast effect is considered, the evaluation of accretion based on Hα strength has a caveat. The chromospheric activity – typically enhanced for young stars – generates a strong Hα emission similar to the case of accretion. The line profile of Hα is used for distinguishing between accreting and non-accreting objects: disc accretion generates broad and asymmetric Hα lines (Luhman et al. 2007). Fig. 2 shows the Hα velocity profiles for 2M1546, which are asymmetric in both two observations. The asymmetric feature can be explained by the inclination effects and/or absorption by an accompanying outflowing wind (Alencar & Basri 2000; Mohanty, Jayawardhana & Basri 2005). A quantitative diagnostic value using Hα emission-line profile is the full width of Hα at 10 per cent of the line peak (v_{10}) (White & Basri 2003; Mohanty et al. 2005). However, the broadened Hα line profile is not always explained by the accretion. Fast rotator and binarity can broaden the Hα emission line, which can be misdiagnosed as an accretor (Manara et al. 2013). In the opposite way, the inclination of the accretion disc can produce a narrower emission line along the line of sight, which can be misdiagnosed as a non-accretor (Mohanty et al. 2005). Published v_{10} accretion criteria vary from $200 < v_{10} < 270$ km s^{-1} (Jayawardhana, Mohanty & Basri 2003; White & Basri 2003; Fang et al. 2013), independent of spectral type. Measured v_{10} values for 2M1546 are over 300 km s^{-1} (Table 1), which exceeds the strictest accretion criterion (i.e. >270 km s^{-1}). Using the v_{10} value and the accretion rate ($\dot{M}_{\rm acc}$) relation of Natta et al. (2004), we estimate $\dot{M}_{\rm acc} = 1.3 \times 10^{-10}$ M$_\odot$ yr^{-1}. Considering many M-type pre-MS stars found to have accretion rates as low as $\sim 2 \times 10^{-12}$ M$_\odot$ yr^{-1} (Herczeg, Cruz & Hillenbrand 2009; Alcalá et al. 2014), the rate we infer for 2M1546 suggests it is actively accreting from its inner disc.

From our SED fitting, we obtain the best-fitting stellar radius (0.461 R$_\odot$), effective temperature (2940 K), and luminosity (0.014 L$_\odot$). We alert readers that this SED fitting ignores any effects from veiling and self-extinction so that they should be taken with caution. Based on Baraffe et al. (2015), these values are inconsistent with values from an ∼55 Myr old M5 star. These best-fitting SED parameters are instead well matched for parameters of a 10 Myr old mid-M type star with mass of 0.1 M$_\odot$. For this mass, a typical mass accretion rate is expected to be 1.0×10^{-10} M$_\odot$ yr^{-1} (Hartmann et al. 2016) that agrees well with our obtained accretion rate. As shown in the following section, 2M1546 is a highly likely member of the 55 Myr old Argus association. When a star has prolonged accretion, then it may be conceivable that such a star has stellar parameters of a younger star because of the accretion effect on its evolution. One needs higher spectal resolution data to confirm this possible effect of accretion by independently obtaining a spectral type not affected by veiling.

Emission in He I λ6678 is also reasonably well correlated with accretion among very low mass stars and brown dwarfs (Mohanty et al. 2005; Alcalá et al. 2014, 2017). Gizis, Reid & Hawley (2002) showed that He I λ6678 is generally present in low levels (|EW(He I)|≪1 Å) in older chromospherically active stars. 2M1546 shows strong He I λ6678 emission at both epochs (EWs of −0.8 and −1.6 Å), supporting the hypothesis of ongoing accretion (See Table 1 and Fig. 4). In addition to strong Hα, we also detect other Balmer line emission up to H17 (Fig. 3).

As shown in Figs 1 and 4, we detect strong [O I] emission at 6300 Å at both epochs. Studies investigating the prominent [O I] λ6300 emission towards young stellar objects suggest that jets, MHD winds, photoevaporative winds, and photodissociation of OH in the disc surface layers are the possible origins of the line (e.g, Stoörzer, Hollenbach & ApJ 2000; Acke, van den Ancker & Dullemond 2005; Rigliaco et al. 2013; Natta et al. 2014; Banzatti et al. 2019). Störzer & Hollenbach (2000) predict that [O I] λ6300 is dominated by OH photodissociation in the region with a line ratio [O I] λ6300/[O I] λ5577 smaller than 10. Our spectra show a potentially weak (∼1 Å) detection of [O I] λ5577 that results in the line ratio of about 3. This small line ratio favours the other explanations for the origin of O I emission such as from winds and/or jets.

3 CIRCUMSTELLAR DISC EMISSION

Dust emission from the circumstellar disc is observed as the IR excess of the SED. The SED of 2M1546 was generated utilizing catalogue data from POSS-II (*JFN*; Cabanela et al. 2003), SkyMapper DR1 (*griz*; Wolf et al. 2018), *Gaia* DR2 ($G_{\rm BP}$, $G_{\rm RP}$, G),

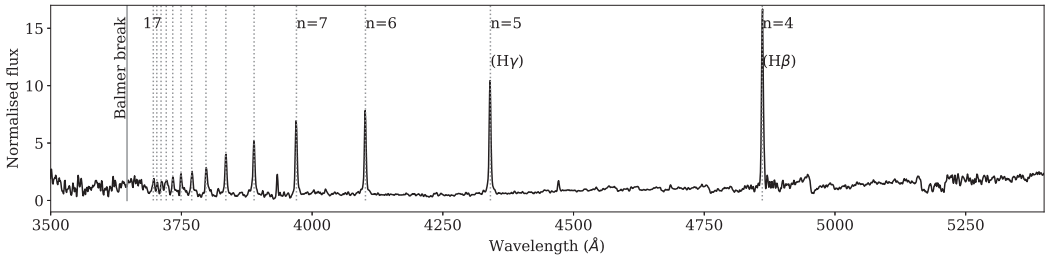

Figure 3. The B3000 spectrum of 2MJ1546 showing Balmer series in emission up to $n = 17$.

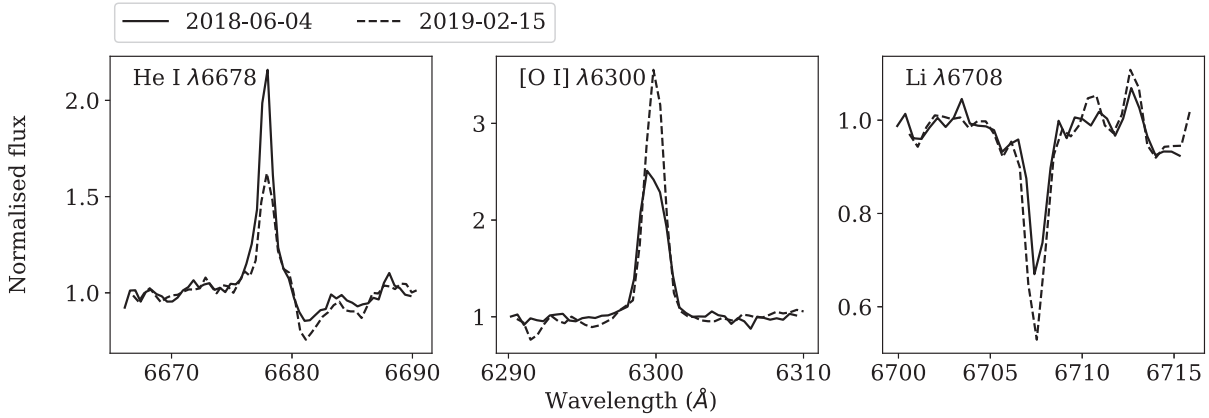

Figure 4. WiFeS/R7000 line profiles of He I λ6678, [O I] λ6300, and Li I λ6708 at the two observation epochs.

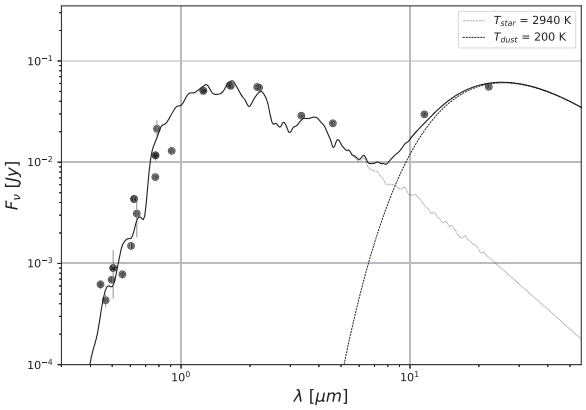

Figure 5. SED for 2M1546 with the best-fitting photosphere model of T_{star} = 2940 K (dotted line) and a 200 K blackbody (dashed line) combined to produce a total model (solid line).

2MASS (*JHK*$_s$; Cutri et al. 2003), and All*WISE* (*W*1 − *W*4; Cutri et al. 2014). Examinations of high angular resolution optical/near-IR images show no possible contaminating source within the spatial resolution of *WISE* images. Therefore, we conclude that there is no contamination and these photometric data are only from 2M1546. We fit synthetic photometry derived from BT-Settl (Allard, Homeier & Freytag 2012) using our SED-fitting technique described in Rhee et al. (2007). The resulting SED and the best-fitting model are presented in Fig. 5.

The best-fitting temperature (T_{star} = 2940 K) is consistent with the pre-MS temperature scale for young (10–30 Myr) stars derived by Pecaut & Mamajek (2013) for a spectral type of M5. We can satisfactorily fit the *WISE W*3 (12 μm) and *W*4 (22 μm) excesses with a single blackbody of temperature $T_{dust} \sim 200$ K. With little excess emission at $\lambda < 5$ μm and a significant excess at $\lambda > 10$ μm we classify 2M1546 as having a transitional disc (Strom et al. 1989; Williams & Cieza 2011), with clearly some material in the inner disc remaining to drive the accretion that we observed.

Murphy et al. (2018) investigated the disc surrounding the M5 Carina member *WISE* J080822.18–644357.3 (hereafter *WISE* J0808), which has a similar SED and accretion characteristics to 2M1546. They found a cold disc component that was well fitted by an ∼240 K blackbody resulting from populations of small dust grains released by sublimating planetesimals. Flaherty et al. (2019) recently observed *WISE* J0808 with the Atacama Large Millimetre/sub-millimetre Array (ALMA) but did not detect any CO gas, indicating *WISE* J0808 may be at an evolutionary state between a gas-rich transition disc and a gas-poor second-generation debris disc. Considering the similarities between *WISE* J0808 and 2M1546, the latter is also probably a borderline transition/debris disc accreting the last of its inner gas on to the star. More observations, including from ALMA, are required before definitively assessing the evolutionary stage of the disc around 2M1546.

4 AGE ESTIMATION BASED ON MOVING GROUP MEMBERSHIP PROBABILITY

One of the key parameters for constraining disc models is stellar age and, for young nearby stars within 150 pc, one of the most reliable age-dating methods is to test whether the star is a member of one of several young moving groups in the solar neighbourhood with well-determined ages (e.g. Zuckerman & Song 2004; Torres et al. 2008). Although the absolute age scales from these moving groups should not be over interpreted, relative age ordering of several major moving groups is secure and can be used to derive ages of member stars at much higher precision than possible for an isolated star. The relative age rank for major moving groups are: TWA < BPMG < Columba/Carina < Argus < AB Dor (Zuckerman & Song 2004; Torres et al. 2008; Gagné et al. 2014; Bell, Mamajek & Naylor 2015). We note that the existence of the Argus group was challenged by Bell et al. (2015) and Riedel et al. (2017), but Zuckerman (2019) reaffirm the Argus moving group.

There are several moving group membership probability calculation tools available in the literature (e.g. BANYAN II and Σ and BAMG 1 and 2; Gagné et al. 2014, 2018; Lee & Song 2018, 2019). The main differences between these tools are their internal membership lists and how they calculate the structural properties (mean *XYZ* positions, *UVW* velocities, and their distributions) of each moving group. BAMG 2 is the most recent code for calculating kinematic memberships and was developed to be self-consistent with respect to group memberships (Lee & Song 2018). For this reason, we adopt membership probabilities from it over those from other tools.

Table 2 presents membership probabilities using our two measured RV values. BAMG 2 evaluates 2M1546 as an Argus member while the two BANYAN models provide a very small Argus membership probability, with the star most likely being a field

Table 2. Kinematic membership probabilities.

	Membership probability: Group (per cent)	
RV (km s^{-1})	-4.4 ± 0.9	-3.5 ± 1
BAMG 2	Argus(95) + Field(5)	Argus(83) + BPMG(14)
BANYAN II	Field(78) + Argus(22)	Field(89) + Argus(9)
BANYAN Σ	Field(94) + Argus(2)	Field(87) + UCL(8) + Argus(5)

Note. Since only groups with membership probabilities >2 per cent are presented here, the sum of probabilities is smaller than 100 per cent.

Table 3. Summary of 2M1546 parameters.

Parameter	Value	Units
RA	15:46:07.52[a]	hh:mm:ss.ss
Dec.	−62:58:04.2[a]	dd:mm:ss.s
SpT	M5	
$\mu_\alpha \cos\delta$	-42.7 ± 0.1[a]	mas yr^{-1}
μ_δ	-61.5 ± 0.1[a]	mas yr^{-1}
Distance	59.2 ± 0.3 [a]	pc
RV	−4.4, −3.5	km s^{-1}
$T_{\rm eff}$	2940	K
log (L/L$_\odot$)	−1.83	dex
$\dot{M}_{\rm acc}$	1.31^{-10}	M$_\odot$ yr^{-1}
Mass	0.11	M$_\odot$
Age	55	Myr
X, Y, Z	45.9, −36.7, −6.7	pc
U, V, W	−16.5, −12.5, −5.6[b]	km s^{-1}
	−15.8, −13.1, −5.7[c]	km s^{-1}

Notes. [a]Gaia Collaboration (2018).
[b]Using RV = −4.4 km s^{-1}.
[c]Using RV = −3.5 km s^{-1}.

object. If 2M1546 was an old field star, then its ongoing accretion is even more interesting yet more challenging to understand. If an isolated accreting pre-MS star, then 2M1546 belongs to a rare group of nearby ($\lesssim$60 pc) youngest stars such as some accreting TWA members. Fig. 6 compares the heliocentric position (XYZ) and velocity (UVW) of 2M1546 to the moving group models used by BAMG 2. The position and velocity of 2M1546 are well matched to the ∼55 Myr-old Argus group, as expected from the membership probabilities in Table 2.

5 DISCUSSION AND CONCLUSIONS

We summarize the important properties of 2M1546 from the literature and this work in Table 3. The proximity (59 pc), late spectral type (M5), old age (55 Myr), mid-IR excess emission, and ample evidence of ongoing accretion observed in 2M1546 make it an interesting laboratory for studying prolonged disc accretion. It is the oldest known accreting star to date, and can therefore be used for studying the upper limit on the lifetimes of gas-rich discs. The kinematic properties of the star are consistent with the Argus moving group and its estimated age of ∼55 Myr.

Over the past several years, several mid-M type accretors at various ages have been reported in the literature (Table 4). All of the stars in Table 4 show strong mid-IR excess emission at *W*3 and *W*4 and signs of ongoing accretion. Among these sources, *WISE* J0808 appears to be the most similar to 2M1546, with v_{10} velocity widths in excess of 300 km s^{-1}. 2MASS J1239–5702 and 2MASS J1422–3623 have slightly weaker Hα equivalent widths and v_{10} values comparble to 2M1546. However, they are believed to be younger (10–17 Myr) members of LCC or UCL subgroups of the Sco–Cen OB association (Murphy, Lawson & Bento 2015). While LDS 5606A+B are also actively accreting sources, they are binaries and hence their accretion might have been affected by their companions. 2MASS J1337–4736 is claimed to be accreting based on its asymmetric Hα profile and *WISE* excess (Rodriguez et al. 2011; Schneider et al. 2012b). Zuckerman (2015) found that this star has a distant companion. While not having a measured v_{10} value, TWA 31 has a strong EW(Hα) value and significant excess at *W*3 and *W*4, supporting an accretion hypothesis (Schneider, Melis & Song 2012a; Zuckerman 2015). The remaining three stars seem to show marginal signs of accretion. 2MASS J0844–7833 and 2MASS J0508–2101 barely exceed the lower limit for accretion criterion in terms of v_{10} and/or EW(Hα). Compared to other accretion sources, 2MASS J0501–4337 also has a significantly lower EW(Hα) and a v_{10} width that barely exceeds the accretion criterion of Barrado y Navascués & Martín (2003).

With the exception of *WISE* J0808, the inferred ages for these stars are all smaller than the age of the β Pic Moving Group ($\lesssim$25 Myr). Therefore, the slightly prolonged accretion at these stars could have been accepted as an unusual phenomenon seen in some rare outliers. Now, we see at least a handful of adolescent mid-M type stars with clear signs of ongoing accretion, suggesting that accretion can be maintained for several tens of million years around low-mass stars under certain conditions. The discovery of these older M-type accretors could eventually reveal a less efficient process of removing circumstellar gas and dust around low-mass stars. We note that the plethora of M5 accretors at ages of 30–55 Myr coincides with the mass boundary at which stars become fully convective in their interiors.

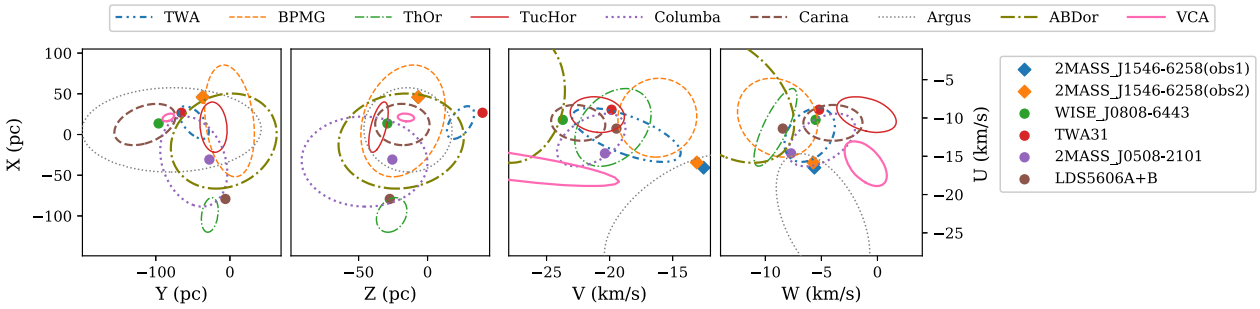

Figure 6. Accreting mid-M type stars and models of NYMGs in the *XYZUVW* spaces.

Table 4. Accreting mid-M type stars from the literature.

Name	SpT	Dist. (pc)	RV (km s^{-1})	EW(H α) (Å)	v_{10} [H α] (km s^{-1})	Age from Lit. (Myr; group)	Age from this work[a] (Myr; group)	Refs.
2MASS J08440915–7833457	M4.5	98	–	60	212	8–14 (ηCha)	–[b]	1
TWA 31	M4.2	81	10.5 ± 0.4	115	–	7–13 (TWA)	7–13 (TWA)	2
2MASS J13373839–4736297	M3.5	126	–	13.7	–	10–17 (LCC)	–[b]	3, 4
2MASS J12392312–5702400	M5	180	16 ± 2	27–63	238–331	10–17 (LCC)	–[b]	5
2MASS J14224891–3623009	M5	–	9 ± 2	33–91	236–341	10–16 (UCL)	–[b]	5
2MASS J05082729–2101444	M5	49	24.9 ± 0.9	25	197	12–25 (BPMG)	30–44 (Columba)	1
LDS 5606 A	M5	84	14.9 ± 0.8	99–135	250	12–25 (BPMG)	30–44 (Columba)	6, 7
LDS 5606 B	M5	84	14.9 ± 0.4	25	135	12–25 (BPMG)	30–44 (Columba)	6, 7
2MASS J05010082–4337102	M4.5	–	–	7.6	210	30–44 (Columba)	–[c]	8
WISE J080822.18–644357.3	M5	90[d]	22.7 ± 0.5	65–125	300–350	30–49 (Carina)	30–49 (Carina)	9
2MASS J15460752–6258042	M5	59	−4.4, −3.5	120–210	310–366	–	40–69 (Argus)	10
J0446A	M6	83	26.7 ± 16.8	10.4	210	30–44 (Columba)	–	11
J0446B	M6	82	29.8 ± 16.8	16.8	239	30–44 (Columba)	–	11
J0949A	M4	79	22.4 ± 16.7	110	367	30–49 (Carina)	–	11
J0949B	M5	78	20.5 ± 16.8	24	305	30–49 (Carina)	–	11

Notes. [a]Ages are obtained based on the moving group membership probabilities calculated using BAMG 2 except where marked.
[b]η Cha, LCC, and UCL are not included in BAMG 2. BANYAN Σ suggests that 2MASS J0844−7833, J1337−4736, J1239−5702, and J1422−3623 are likely members of η Cha ($P = 62$ per cent), LCC ($P = 63$ per cent), LCC ($P = 52$ per cent), and UCL ($P = 84$ per cent), respectively.
[c]Since a *Gaia* proper motion for this star not exist, the Bayesian membership probability cannot be calculated.
[d]Kinematic distance based on membership in Carina (Murphy et al. 2018).
Notes. References for group age: η Cha – Bell et al. (2015); TWA – Bell et al. (2015); LCC – Song, Zuckerman & Bessell (2012), Pecaut & Mamajek (2016); UCL – Song et al. (2012), Pecaut & Mamajek (2016); BPMG – Song & Zuckerman (2003), Bell et al. (2015); Columba – Torres et al. (2008), Bell et al. (2015); Carina – Torres et al. (2008), Bell et al. (2015); Argus – Bell et al. (2015), Zuckerman (2019).
References. (1) Schneider et al. (2019); (2) Schneider et al. (2012a); (3) Schneider et al. (2012b); (4) Rodriguez et al. (2011); (5) Murphy et al. (2015); (6) Rodriguez et al. (2014); (7) Zuckerman, Vican & Rodriguez (2014); (8) Boucher et al. (2016); (9) Murphy et al. (2018); (10) This work.; (11) Silverberg et al. (2020).

ACKNOWLEDGEMENTS

We thank Michael Bessell for obtaining the second epoch B3000 and R7000 spectra of 2M1546 in 2019 February. This work was supported by the Basic Science Research Program through the National Research Foundation of Korea (Grant no. NRF-2018R1A2B6003423).

REFERENCES

Acke B., van den Ancker M. E., Dullemond C. P., 2005, A&A, 436, A209
Alcalá J. M. et al., 2014, A&A, 561, A2
Alcalá J. M. et al., 2017, A&A, 600, A20
Alencar S., Basri G., 2000, AJ, 119, 1881
Allard F., Homeier D., Freytag B., 2012, Phil. Trans. R. Soc. A., 370, 2765
Antoniucci S. et al., 2011, A&A, 534, A32
Banzatti A., Pascucci I., Edwards S., Fang M., Gorti U., Flock M., 2019, ApJ, 870, 76
Baraffe I., Homeier D., Allard F., Chabrier G., 2015, A&A, 577, A42
Barrado y Navascués D., Martín E. L., 2003, AJ, 126, 2997
Basri G., Marcy G. W., 1995, AJ, 109, 762
Bell C. P. M., Mamajek E. E., Naylor T., 2015, MNRAS, 454, 593
Biazzo K., Alcalá J. M., Frasca A., Zusi M., Getman F., Covino E., Gandolfi D., 2014, A&A, 572, A84
Bochanski J., West A., Hawley L., Covey R., 2007, AJ, 133, 531
Boucher A., Lafrenière D., Gagné J., Malo L., 2016, ApJ, 832, 50
Cabanela J. E., Humphreys R. M., Aldering G., Larsen J. A., Odewahn S. C., Thurmes P. M., Cornuelle C. S., 2003, PASP, 115, 837
Childress M. J., Vogt F. P. A., Nielsen J., Sharp R. G., 2014, Ap&SS, 349, 617
Cutri R. M. et al., 2003, 2MASS All Sky Catalog of Point Sources, VizieR On-line Data Catalog: II/246
Cutri R. M. et al., 2014, AllWISE Data Release, VizieR Online Data Catalog: II/328
Dopita M., Hart J., McGregor P., Oates P., Bloxham G., Jones D., 2007, Ap&SS, 310, 255
Duchêne G., Becker A., Yang Y., Bouy H., De Rosa R., Patience J., Girard J. H., 2017, MNRAS, 469, 1783
Fang M., Kim J. S., van Boekel R., Sicilia-Aguilar A., Henning T., Flaherty K., 2013, ApJS, 207, 5
Flaherty K., Hughes A. M., Mamajek E. E., Murphy S. J., 2019, ApJ, 872, 92
Gagné J., Lafrenière D., Doyon R., Malo L., Artigau É, 2014, ApJ, 783, 121
Gagné J. et al., 2018, ApJ, 856, 23
Gaia Collaboration, 2018, A&A, 616, 1
Gizis J. E., Reid I. N., Hawley S. L., 2002, AJ, 123, 3356
Greaves J. S., Rice W. K. M., 2010, MNRAS, 407, 1981
Haisch K. E. Jr, Lada E. A., Lada C. J., 2001, ApJ, 553, 153
Hartmann L., Herczeg G., Calvet N., 2016, ARA&A, 54, 135
Herczeg G., Hillenbrand L. A., 2008, ApJ, 681, 594
Herczeg G., Cruz K. L., Hillenbrand L. A., 2009, ApJ, 696, 1589
Ingleby L., Calvet N., Hernández J., Hartmann L., Briceno C., Miller J., Espaillat C., McClure M., 2014, ApJ, 790, 47
Jayawardhana R., Mohanty S., Basri G., 2003, ApJ, 592, 282
Lee J., Song I., 2018, MNRAS, 475, 2955
Lee J., Song I., 2019, MNRAS, 486, 3434
Luhman K. L., Joergens V., Lada C., Muzerolle J., Pascucci I., White R., 2007, Protostars and Planets V. University of Arizona Press, Tucson, p. 443
Mamajek E. E., 2009, in Usuda T., Tamura M., Ishii M., eds, AIP Conf. Proc. Vol. 1158, Exoplanets And Disks: Their Formation And Diversity. Am. Inst. Phys., New York, p. 3
Mamajek E. E., Meyer M. R., Liebert J., 2002, AJ, 124, 1670
Manara C. F. et al., 2013, A&A, 551, A107
Manara C. F., Morbidelli A., Guillot T., 2018, A&A, 618, A3
Martín E., Montmerle T., Gregorio-Hetem J., Casanova S., 1998, MNRAS, 300, 733
Miszalski B., Mikołajewska J., 2014, MNRAS, 440, 1410
Mohanty U., Jayawardhana R., Basri G., 2005, ApJ, 626, 498

Moór A. et al., 2011, ApJ, 740, L7
Murphy S. J., Lawson W. A., Bento J., 2015, MNRAS, 453, 2220
Murphy S. J., Mamajek E. E., Bell C. P. M., 2018, MNRAS, 476, 3290
Muzerolle J., Hartmann L., Calvet N., 1998, AJ, 116, 2965
Najita J. R., Kenyon S. J., 2014, MNRAS, 445, 3315
Natta A., Testi L., Muzerolle J., Randish S., Comerón F., Persi P., 2004, A&A, 424, A603
Natta A., Testi L., Alcalá J. M., Rigliaco E., Covino E., Stelzer B., D'Elia V., 2014, A&A, 569, A5
Pecaut M. J., Mamajek E. E., 2013, ApJS, 208, 9
Pecaut M. J., Mamajek E. E., 2016, MNRAS, 461, 794
Pfalzner S., Bannister M. T., 2019, ApJ, 874, 34
Rhee J. H., Song I., Zuckerman B., McElwain M., 2007, ApJ, 660, 1556
Ribas Á., Bouy H., Merín B., 2015, A&A, 576, A52
Riedel A. R., Blunt S.C, Lambrides E. L., Rice E. L, Cruz K. L., Faherty J. K., 2017, AJ, 153, 95
Rigliaco E., Pascucci I., Gorti U., Edwards S., Hollenbach D., 2013, ApJ, 772, 60
Rodriguez D. R., Zuckerman B., Kastner J. H., Bessell M. S., Faherty J. K., Murphy S. J., 2013, ApJ, 774, 101
Rodriguez D. R., Zuckerman B., Faherty J. K., Vican L., 2014, A&A, 567, A20
Schneider A. C., Melis C., Song I., 2012a, ApJ, 754, 39
Schneider A. C., Song I., Melis C., Zuckerman B., Bessell M., 2012b, ApJ, 757, 163
Schneider A. C., Shkolnik E. L., Allers K. N., Kraus A. L., Liu M. C., Weinberger A. J., Flagg L., 2019, AJ, 157, 234
Silverberg S. M. et al., 2016, ApJ, 830, L28
Silverberg S. M. et al., 2020, ApJ, 890, 106
Song I., Zuckerman B., 2003, ApJ, 599, 342
Song I., Zuckerman B., Bessell M. S., 2012, AJ, 144, 8
Stoörzer H., Hollenbach D., 2000, ApJ, 539, 751
Strom K. M., Strom S. E., Edwards S., Cabrit S., Skrutskie M. F., 1989, AJ, 97, 1451
Torres C. A. O., Quast G. R., Melo C. H. F., Sterzik M. F., 2008 , Handbook of Star Forming Regions, Vol. II. 5, p. 757
Vacca W. D., Sandell G., 2011, ApJ, 732, 8
White R. J., Basri G., 2003, ApJ, 582, 1109
Williams J. P., Cieza L. A., 2011, ARA&A, 49, A67
Wolf C. et al., 2018, Publ. Astron. Soc. Aust., 35, 10
York D. G. et al., 2000, AJ, 120, 1579
Zuckerman B., 2015, ApJ, 798, 86
Zuckerman B., 2019, ApJ, 870, 27
Zuckerman B., Song I., 2004, ARA&A, 42, A685
Zuckerman B., Song I., 2012, ApJ, 758, 77
Zuckerman B., Vican L., Rodriguez D. R., 2014, ApJ, 788, 102

This paper has been typeset from a TEX/LATEX file prepared by the author.